Post-print on Author's Personal Website: James C Koch

Article Name with DOI link to post-print published Version complete citation:

- Gargoum, Suliman A. and Karsten, Lloyd and El-Basyouny, Karim and Koch, James C. Automated assessment of vertical clearance on highways scanned using mobile LiDAR technology. Automation in Construction. 95: 260-274. http://www.sciencedirect.com/science/article/pii/S0926580517310014

Article Post-print starts on the next page →

Automation in Construction 95 (2018) 260–274

Contents lists available at ScienceDirect

Automation in Construction

journal homepage: www.elsevier.com/locate/autcon

Automated assessment of vertical clearance on highways scanned using mobile LiDAR technology

Suliman A. Gargoum*, Lloyd Karsten, Karim El-Basyouny, James C. Koch

Department of Civil and Environmental Engineering, University of Alberta, Edmonton, AB T6G 1H9, Canada

ARTICLE INFO

Keywords:
Lidar point cloud
Bridge inspection
Vertical clearance
Bridge clearance
Automated clearance assessment
Overhead object detection

ABSTRACT

Assessing vertical clearance at bridges is a preliminary step in most routine bridge inspections. This information is critical when assessing the structural integrity of bridges. Furthermore, clearance information at bridges and other overhead assets on a highway network is also extremely important when routing oversized vehicles on a highway network. Efficient clearance assessment makes critical information readily available to asset owners. As a result, asset owners and transportation agencies are able to address concerns in a timely manner, which would help them avoid prohibitive maintenance costs sustained in case of collisions. Unfortunately, manual clearance assessment using conventional surveying tools is unsafe, time consuming, labour intensive. To overcome these challenges, this paper proposes a novel algorithm whereby mobile LiDAR data could be used to efficiently assess clearance at overhead objects on highways. The proposed algorithm first detects and classifies all overhead objects on a highway segment. The clearance is then assessed at each of those objects and minimum clearance is identified. Detection involves voxel-based segmentation of the point cloud followed by a nearest-neighbour search to locate overhead structures. After detecting the structures and identifying their locations, points representing the same object are clustered and classify into bridges and non-bridges. Furthermore, an estimate of the clearance at each object is also obtained. For objects of long span such as bridges, detailed clearance assessment is performed. The developed algorithm was tested on three highway segments in Alberta, Canada including a 242 km highway corridor. Testing revealed that the method was successful in detecting and classifying all overhead structures at an accuracy level of 97.8% and 96.2%, respectively. The algorithm was also successful in accurately measuring the clearance at those structures with the differences in measurement between ground truth data and the extracted results ranging between 0.03 and 0.47%.

1. Introduction

It is common practice for Departments of Transport (DOT) to keep inventory information about all overhead assets on a highway, including bridges, powerlines and overhead signs. Vertical clearance information at those objects must also be obtained to ensure that minimum clearance requirements are met. In fact, current bridge management practice includes a routine inspection phase where a diagnosis of the current state of the structure is obtained [1–3]. Clearance information is collected periodically as part of those bridge inspection procedures since structural degradation and environmental conditions might cause changes to minimum clearance at overhead assets on highways. Such problems should be addressed in a timely manner.

Vertical clearance information at both bridges and powerlines is also essential to agencies responsible for issuing overheight permits for oversized vehicles. The efficiency and accuracy in which such information could be obtained helps significantly improve the effectiveness of routing oversized vehicles on a highway network. In contrast, inaccurate clearance information could result in the risk of collisions or significant delays to the routing program and hectic maintenance costs in cases of bridge strikes [4]. In fact, Bridge strikes are a common problem all around the world [5]. In the US, the Federal Highway Administration ranks damage due to bridge-vehicle collision as the third most common cause of bridge failure [6]. Similarly, statistics from Beijing, China, show that 20% of damage to bridges is caused by bridges being struck by overheight vehicles [7]. In the UK, national statistics show that a vehicle strikes a railway bridge every four and a half hours [5]. In California, the rate of bridge strikes averages a single strike per month [8]. Unfortunately, repairing the damage caused by bridge-vehicle collisions can pose a significant financial burden on

* Corresponding author.
E-mail addresses: gargoum@ualberta.ca (S.A. Gargoum), lkarsten@ualberta.ca (L. Karsten), basyouny@ualberta.ca (K. El-Basyouny), jckoch@ualberta.ca (J.C. Koch).

https://doi.org/10.1016/j.autcon.2018.08.015
Received 7 November 2017; Received in revised form 18 July 2018; Accepted 28 August 2018
Available online 04 September 2018

transportation agencies. For instance, the Texas Department of Transportation reports that bridge strike each incident costs an average $180,000 USD to repair [5].

Although the most significant damage is incurred when oversized vehicles strike bridges, potential conflicts also exist between oversized vehicles and other overhead, Vasquez [9] describes evaluating obstructions along a 15 mile route along which Space Shuttle was to be transported in Los Angeles, California. Over 700 conflicts were detected (155 of which were with powerlines). This information was then used by utility companies plan ahead and clear the route.

In addition to helping agencies issue overheight permits to oversized vehicles, clearance information at bridges and powerlines is also critical to agencies responsible for designating high-load corridors where clearance is expected to exceed a certain margin (9 m in Alberta) along the entire highway.

Unfortunately, in current surveying practice conducting clearance assessment is a time consuming, labour intensive and financially demanding exercise. This makes network-wide assessments of all overhead assets extremely challenging, particularly in places like the Province of Alberta in Canada where a large highway network (31,000 km) exists with approximately 4500 bridge structures and tens of thousands of powerlines and overhead signs [10]. In fact, the size of the network forces officials to set priorities when managing assets on their highways. In case of bridges, this is achieved by performing prioritizing structures which are in a critical condition or focusing on structures located on primary highways [11].

Considering the fact that around 40% of the bridges currently in use in Canada and the US were built over 50 years ago [12], a significant number of these structures are approaching critical conditions and require timely strengthening, rehabilitation, or replacement [13,14]. Unfortunately, given the limitations of existing data collection techniques, assessing clearances at all those structures simultaneously is not feasible. To increase the efficiency of vertical clearance assessment, transportation agencies have considered the use of digital rods and static Light Detection and Ranging (LiDAR) equipment [15]. Although such techniques increase the accuracy of the measurements by minimizing human error, site visits and road closure are still required to perform such assessments due to the manual nature of collecting such data.

This paper proposes a novel algorithm for the automated detection and clearance assessment of overhead assets on highways scanned using mobile LiDAR remote sensing technology. Mobile LiDAR datasets consist of closely spaced points forming an accurate 3D model of a highway. Unlike static terrestrial laser scanning and other conventional surveying tools, Mobile Laser Scanning (MLS) equipment is mounted on a vehicle which collects data while travelling down a road at highway speeds. This causes minimal disruption to traffic and increases the efficiency of the data collection process. Time savings of days, weeks, and months (depending on the size of the project) have all been reported in previous research [16].

As the data collection truck travels down the highway, the laser scanner emits millions of light beams per second at surrounding objects. These light beams reflect back to the scanning system and based on the reflection time and energy, intensity and positional information about points on the object off which the bean was reflected can be computed. The scanning process creates a 360^0-virtual point cloud data of the highway such as that seen in Fig. 1. Such point cloud data can be used to extract traffic sign inventory and lane markings [17–19] as well as several geometric features of highways and other elements of civil infrastructure [20–27]. Laser scanning data has also been used in sight distance assessments [28,29]. MLS provides detailed data, which makes it the most common approach to collect LiDAR data for transportation applications [16]. Unlike traditional surveying methods, the use of LiDAR data enables vertical clearance assessments at any point beneath overhead structures due to the high point density of the cloud data. Since clearances typically vary at different points beneath bridges, using LiDAR data increases the likelihood of identifying the actual minimum clearance under a bridge.

The algorithm proposed in this paper involves automating the detection of overhead objects on a highway segment and identification of clearance information for each of the objects in an efficient and accurate manner, this provides transportation agencies with information that could help them reduce the risk of potential bridge strikes through timely intervention to address structural imperfections and though the efficient routing of oversized vehicles on the highway network. Since incorporating new technologies into protocols requires validation, the accuracy and repeatability of the algorithms was tested on three different highway segments including a 242 km corridor.

2. Previous work

Various techniques have been used to conduct vertical clearance assessments on highways. Although some municipalities still use manual methods, such as theodolites and total stations, other digitized devices have recently gained popularity. For instance, many DOTs use digital measuring rods and electronic measuring devices [30], similarly, clearance assessment using photolog data has also been previously attempted [31]. Terrestrial LiDAR scanning is another technique which has been used to assess clearance at bridges with the aim of minimizing human error associated with conventional surveying tools.

In a paper by Liu, et al. [15], static terrestrial LiDAR scans of a bridge deck and the ground points beneath the deck were used to assess vertical clearance. The authors developed an algorithm where scanned ground points are automatically matched to bridge deck points which fall within a certain margin of the vertical plane that is perpendicular to the ground surface. The algorithm loops through all points until all points on the ground surface are matched to points on the bridge deck.

Riveiro, et al. [2] proposed a method by which photogrammetric images could be used to conduct clearance assessment at bridges. After converting the images into a 3D point cloud, the authors propose assessing the clearance based on a 3D curve fitting algorithm. The procedure involves using points on the pavement surface to create a 3D plane that fits the road surface, where the normal vector to the plane specifies the vertical direction from the roads surface. The vector along the bridge beam's primary axis and the normal vector of the roads surface are used to define a new plane and clearance is measured within that plane. The proposed method was tested on a bridge in New Mexico, USA. To test the accuracy of the proposed method, the authors measured clearance at multiple points below the test bridge. For each point the clearance measurement was obtained using both (1) the proposed photogrammetric technique, and (2) topographical data obtained in field measurements. The difference between the two measurements at each point was then computed and averaged across all points. The average difference was 0.008 m.

In general, digitized vertical clearance assessment techniques such as static LiDAR scanning increase the likelihood of determining the actual minimum clearance beneath a bridge. However, due to the static nature of such tools, disruptions to traffic and safety concerns are common occurrences which still exist. Moreover, network-level analysis (i.e. assessing a large selection of bridges on the network efficiently) is still not possible since such techniques involve conducting site visits and scanning each bridge in the network individually as well as manually.

In a recent paper, Puente, et al. [32], used mobile LiDAR data in the assessment of vertical clearance in tunnels. The authors propose a semi-automated algorithm where cross sections along the trajectory of the tunnel are first extracted and then used to measure the clearance. The method involves using lane markings to define the edges of the travel lanes at which the clearance must be evaluated. The edges are then matched with the points at the roof of the tunnel and the cross section of the tunnel is defined using a convex hull before measuring the clearance. The results were extremely encouraging, with relative error

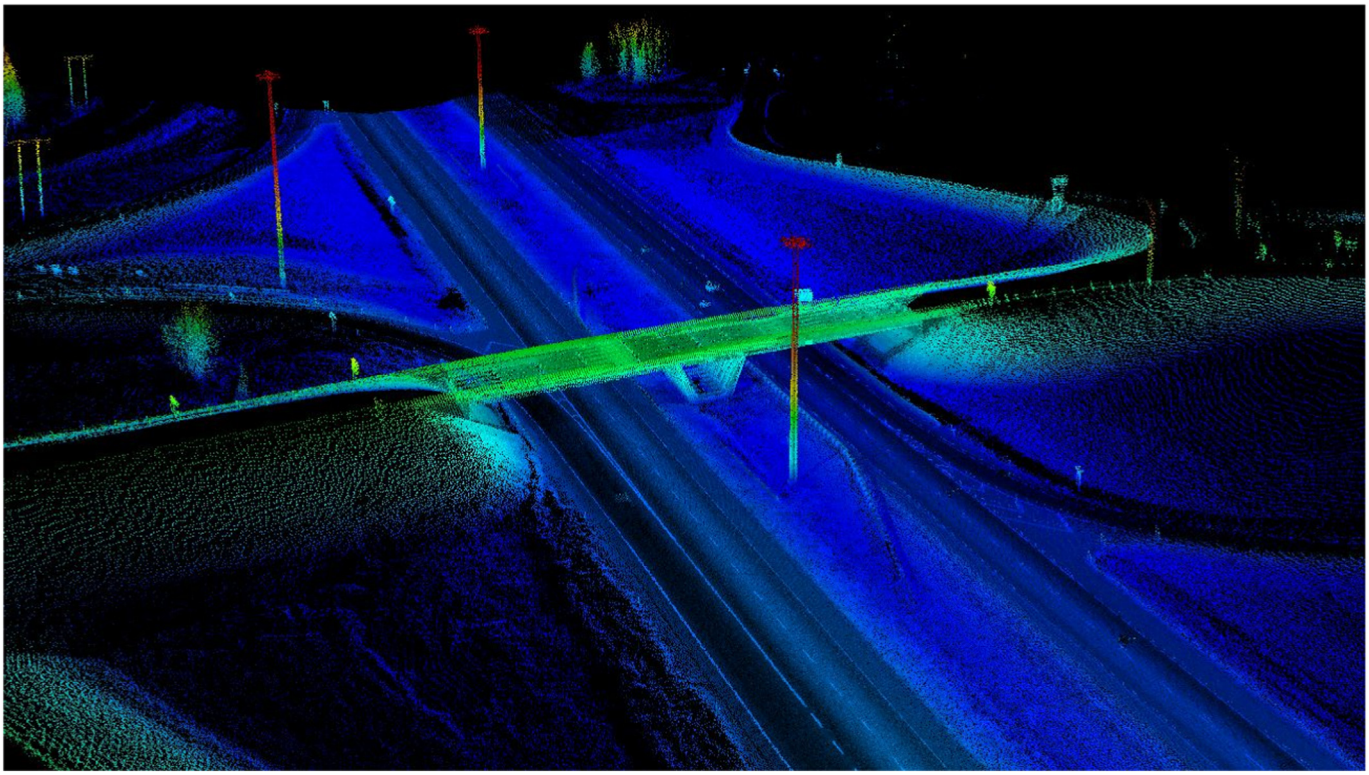

Fig. 1. Point cloud highway.

between ground truth and detected clearance not exceeding 1% for most cross sections. It is worth pointing out that the algorithm was only used to assess a portion of the point cloud data available, with the authors citing loading time as the main reason why the full point cloud was not used to test the algorithm.

As evident from the review, not many studies have attempted measuring vertical clearance of bridges using mobile LiDAR data. Furthermore, to the best of the authors' knowledge, no study, to date, has attempted the automated detection (i.e. inventory) of bridges on highways. Moreover, previous research seems limited to using LiDAR data in assessing clearance of bridges only, with no attention given to other overhead objects such as the power lines and overhead signs as seen in Fig. 2. To address the aforementioned gaps in the literature, this paper develops an automated algorithm which can detect and measure vertical clearance of all overhead objects using mobile LiDAR data.

3. Extraction procedure

The technique proposed for extracting vertical clearance information from LiDAR data involves detecting and classifying overhead structures while obtaining an estimate of their vertical clearance. After that a detailed assessment of vertical clearance at the detected overhead objects is performed. The next few paragraphs provide detailed description of the different steps in extraction procedure. Moreover, the workflow is also summarized in the Fig. 3.

3.1. Overhead structure detection

Detection of overhead structures before measuring their clearance is essential when a network-wide assessment of vertical clearance is desired or when agencies are only interested in inventorying the number of overhead structures that exist on a highway segment. The aim is to minimize the need for user input and to automatically provide information about of the locations where overhead structures exist. Once this is achieved, a detailed assessment of vertical clearance can be performed if desired.

3.1.1. Trajectory definition

The first step of the detection process involves defining points parallel to the roads axis which trace the roads trajectory and cover the entire road segment. In case of this study, the set of points tracing the path of the data collection truck were used. These points were obtained by filtering the LiDAR point cloud based on the scanner angle in MATLAB. Specifically, points that fall in the Nadir plane of the laser scanner were filtered out of the LiDAR point cloud to represent the points parallel to the road's axis. It is worth noting here that the trajectory points extracted in this stage do not need to trace the centreline of the road or the lane. The only requirement is that the points run parallel to the road's axis and extend throughout the entire segment. The location of the trajectory points is only significant if the detection of objects that overhang from the side of the road is desired. This includes overhead signs that only extend into a single lane and do not span across the entire road. If the detection of such an object is desired, it is recommended that the trajectory points are offset into the desired lane before running the remainder of the detection algorithm.

3.1.2. Point cloud segmentation

Once the trajectory points are defined, the next step is to segment the point cloud whereby points that potentially represent overhead objects are filtered out of the remainder of the LiDAR point cloud. In brief, the segmentation procedure involves voxelisation of the LiDAR point cloud and dynamically filtering points that potentially represent overhead objects from the remainder of the point cloud. Voxelisation is the process of discretizing the LiDAR point cloud into three dimensional voxels of a certain size, similar to two-dimensional pixels in a normal two-dimensional image. Interested readers are referred to [33,34] for more information about the voxelization process.

The dimensions of the voxel are user defined. For best overall results, it is recommended that voxel dimensions be defined based on the laser scanner properties. Since the data scanned in this study was

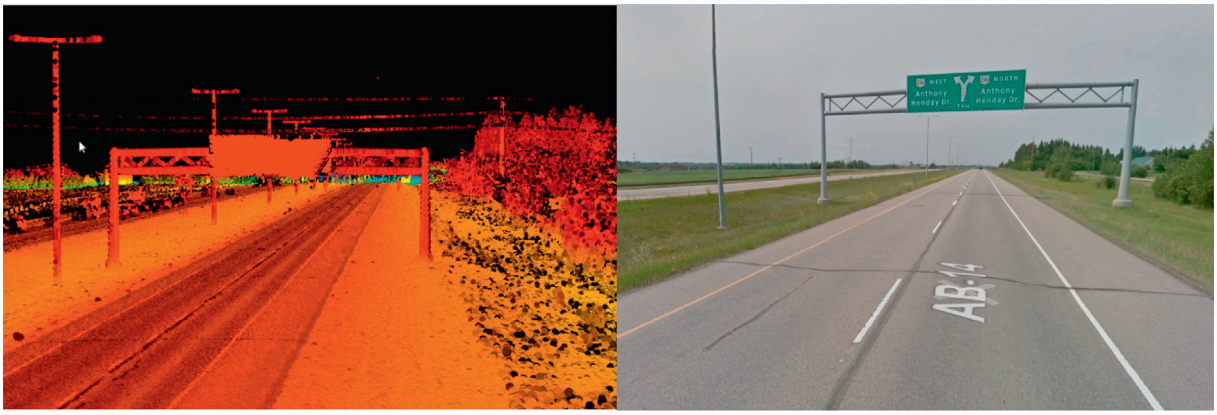

(a) Overhead Sign

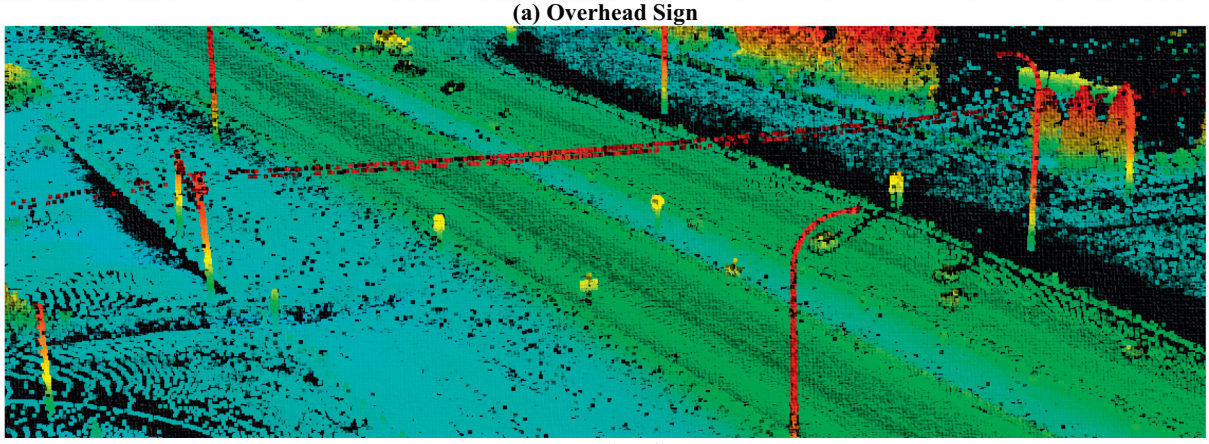

(b) Powerline Cable

Fig. 2. Overhead objects.

collected in scanlines that are approximately 20 cm apart, a similar cell size for voxelization was used. This choice also enables efficient creation of 3D images within the limits of 16GB of RAM.

After discretizing the LiDAR point cloud into a 3D voxel grid, the data was segmented based on the elevation of each point from the road surface. This was done to isolate points representing potential overhead objects from the remainder of the point cloud.

To account for variations in the vertical alignment along the highway, the threshold was applied dynamically (i.e. a different reference point on the pavement surface was used to classify points depending on where the point is located along the road segment). The reference point for each point in the point cloud was the closest voxel in the trajectory voxel chain shown in Fig. 4.

To achieve this, a nearest neighbour search was conducted for each point in the point cloud. Once the closest voxel for every point is identified, the elevation difference between each point and that trajectory voxel is then computed. Points that have an elevation difference which is more than a specific threshold are then classified as potential overhead object candidates and are retained for the object detection step in Section 3.1.3. The classification threshold is user defined depending on where the split is desired. A 3 m threshold was used in this paper since this retains all points representing overhead structures while minimizing the search space for the object-detection step as evident in Fig. 5.

3.1.3. Object detection

The third step of the detection process involves matching the trajectory data with the overhead object candidate points obtained in the previous step to locate the overhead structures. At every point along the defined trajectory, a nearest neighbour search algorithm was used to locate any overhead structures above the trajectory point [35]. As displayed in Fig. 6, the aim is to search for the nearest overhead point to the trajectory point on the ground.

The MATLAB algorithm loops through all trajectory points (pins shown in Fig. 6) and returns a list of points for which an overhead match was found. For instance, for the dashed arrow in Fig. 6, no overhead points exist above the trajectory points, therefore, no overhead object is detected. However, for the solid line, overhead points representing a power line exist above the trajectory pin and hence, the code identifies this as a location where an overhead structure does exist. The code also computes the difference in elevation between the overhead point and the point on the road's surface (i.e. the trajectory point). This estimate is used as a preliminary estimate of the clearance at that location.

For overhead objects which have a limited thickness, and as a result, a low point density (along the road's axis) (< 3), an additional check is conducted to ensure that the detected overhead points are indeed part of an overhead object and not random points representing noise. This is done by assessing the existence of points within the lateral vicinity of the detected point. Specifically, a search is conducted for points which were closest to the detected overhead point in the lateral direction (i.e. the direction perpendicular to the road's axis), as shown in Fig. 7.

The average distance from cluster of 10 nearest points, p_n to the point p_i is determined and is assessed follows.

$$\begin{aligned} &\overline{Y_i} < 1m \rightarrow \text{is an overhead object} \\ &\overline{Y_i} \geq 1m \rightarrow \text{is noise} \end{aligned} \tag{5}$$

where $\overline{Y_i}$ is the mean distance from the 10 nearest neighbouring points p_n to the original overhead point p_i. It is assumed here that if the points are scattered > 1 m away then it is highly unlikely that these points belong to the same overhead object and, hence, the detected point does not represent an overhead object.

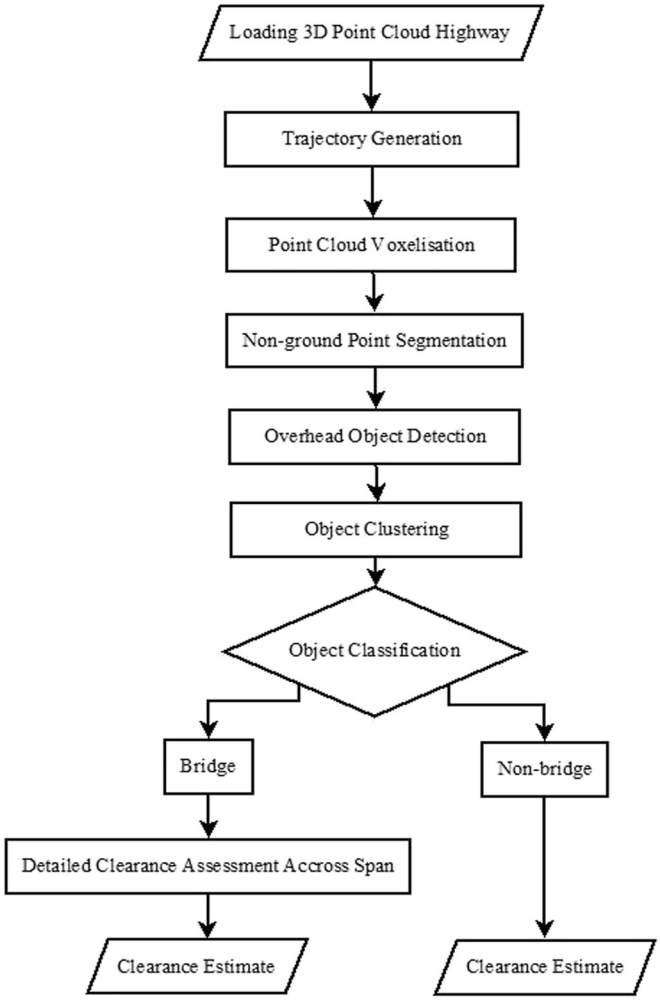

Fig. 3. Procedure workflow.

The reason a 1 m and 10 point threshold was chosen is because the minimum point density of data used in this study is approximately 100 points per square meter. Assuming the points are evenly distributed along either end of the square meter, this translates to approximately 10pts/m. It is worth noting here that sensitivity analysis was conducted for the distance and point density thresholds and it was found that these thresholds did not impact detection accuracy. It is also worth emphasizing that this is an additional filter that is only applied to help distinguish overhead objects with a low point density from noise.

3.1.4. Clustering & classification

To identify the number of overhead structures determined on a segment, trajectory points along the roads surface for which a match was found are clustered using the DBSCAN (Density-Based Spatial Clustering of Applications with Noise) clustering algorithm [36].

The DBSCAN algorithm is a density-based algorithm that works on grouping points based on proximity (Ɛ) and hit count. The proximity measure defines how close multiple points within a cluster are to one another. Hit count is a measure of the minimum number of points required for those points to be considered a cluster. If the distance between points exceeds the minimum proximity (Ɛ) and the number of points exceeds the minimum hit count, it is likely that these points do not represent a cluster. In this paper, a minimum hit count of 4 and a proximity (Ɛ) of 1 m were used to group of points into clusters, or in this case, an overhead object.

DBSCAN was selected for two main reasons. (i) DBSCAN does not require specifying the number of clusters in advance which is extremely important for this application since we assume the number of overhead objects is unknown. (ii) DBSCAN has the ability to account for noise and does not require that all points are assigned to clusters, which means that outliers are ignored. This helps improve the accuracy of the detection and classification process by removing erroneous points.

Classification of clusters into bridges and non-bridges is done by applying two different statistical filters that are related to the density and spread of points in a cluster. Before discussing the filters, it is worth noting that objects were only classified into bridges and non-bridges since this is the most important distinction for transportation agencies interested in obtaining clearance information for bridge inspections. It is recommended that future research explores further classification of non-bridges into specific objects such as powerlines and vegetation. Such classification although possible is out of the scope of this paper.

Due to the wide span on bridges, point density of clusters detected along their cross sections is relatively high compared to other overhead objects such as powerlines. As a result, it is expected that points along a bridge's cross section in the x-y plane would fit very well to a linear model as evident in Fig. 8. In contrast the sparse and random nature of points along a powerline's cross section means that they would generally fit poorly to a linear model. Therefore, the first classification filter is based on how well the points in a cluster fit a linear model in the x-y plane. For objects where model fit is high (i.e. R-squared > 0.7) [37], these objects are bridge candidates however, they are subject to a second filter before they could be classified as bridges.

The second classification filter is related to the geometric distribution of the residuals of the regression model. As evident in Fig. 9, the high density of points detected along a bridge's cross sections results in the probability density plot of the residuals peaking at the mean of zero. The Kurtosis, which is also known as the 4th central moment around the mean, is used to assess the peak in the residual density plot. Kurtosis parameter (γ) can be quantified as follows:

$$\gamma = \frac{n\sum_{i=1}^{n}(x_i - \overline{X})^4}{\left(\sum_{i=1}^{n}(x_i - \overline{X})^2\right)^2} \tag{6}$$

where, x_i is the residual of point (i), $\overline{X}$ is the mean of all residuals, n denotes the number of observations in the cluster.

A sample with a parameter = 3 is considered normally distributed. If $\gamma < 3$ then the sample is a leptokurtic (peaked) sample, on the other hand, if $\gamma > 3$ then the sample is a platykurtic (flat) sample [38]. Therefore, clusters with a high linear model fit and a high kurtosis ($\gamma > 3$) are considered bridge clusters.

Finally, for all clusters which are determined to be overhead objects, the algorithm returns a clearance measurement at the point of detection. Although this measurement does not cover the all spans of the overhead object, it gives the user an estimate of the vertical clearance of the object in question.

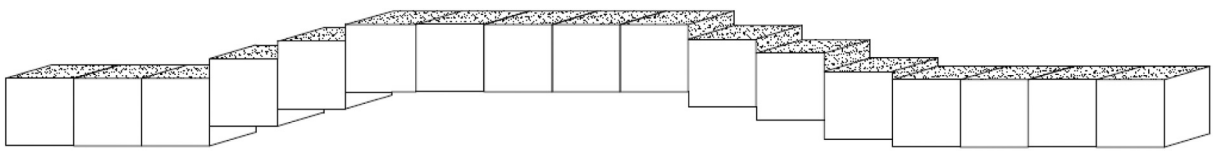

Fig. 4. Side view of the trajectory voxel chain tracing the road's axis along pavement surface.

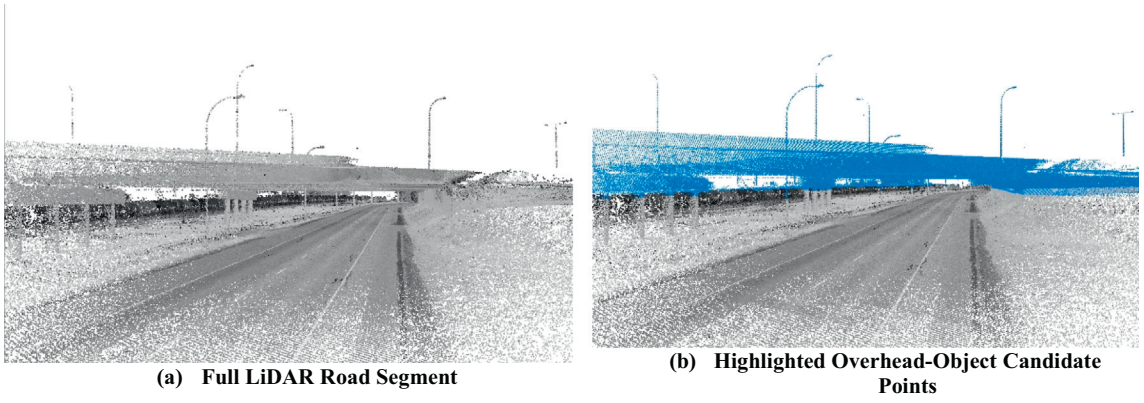

(a) Full LiDAR Road Segment

(b) Highlighted Overhead-Object Candidate Points

Fig. 5. Point cloud segmentation.

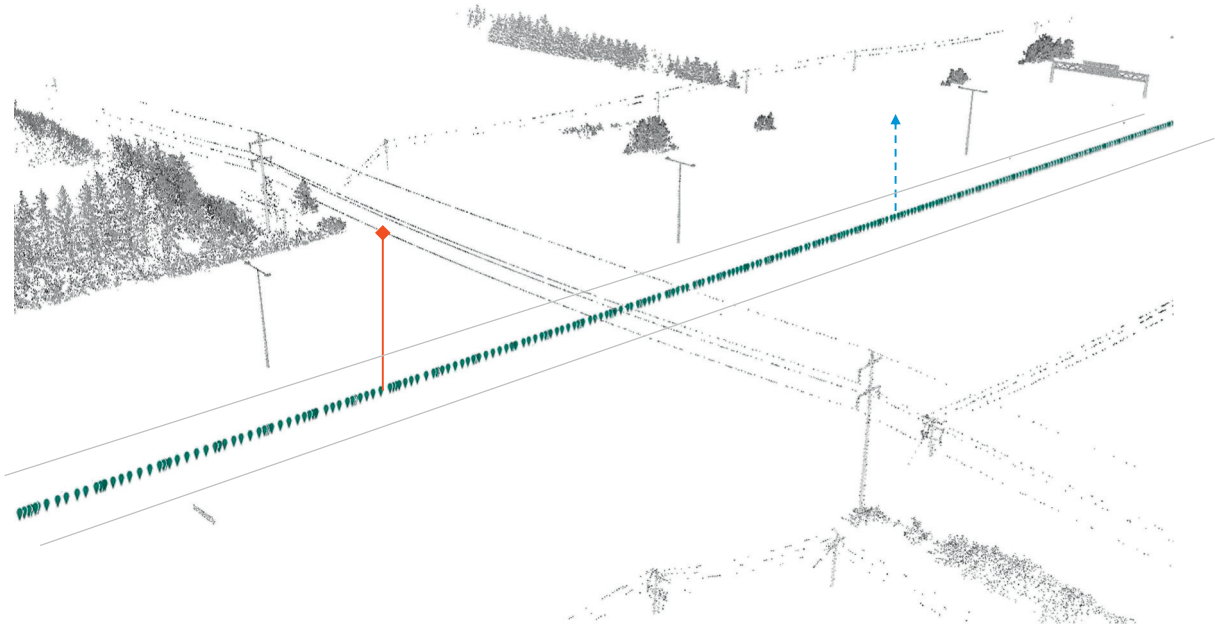

Fig. 6. Overhead object detection (No overhead points exist above the trajectory points at the dashed arrow upstream the segment, therefore, no overhead object is detected. For the solid line overhead points representing a power line exist above the trajectory pin and hence, an overhead object is detected).

3.2. Detailed clearance assessment

To obtain a more detailed estimate of clearance on bridge structures where vertical clearance could vary at different points along the bridge's span, a detailed clearance assessment is recommended. The detailed assessment involves replicating the trajectory points used in the overhead object detection across the width of the road and matching the new set of trajectory points with points on the bridge structure using nearest neighbour search. As seen in Fig. 10, this guarantees accurate clearance measurements when the pavement surface has a high cross slope or when then road has a high grade.

Since different agencies require clearance measurements at different locations below a bridge structure, the specific points at which the clearance is assessed are left for the user to specify. In the example presented as part of the case study (Section 5.2.2), clearance is assessed in different lanes, on different approaches, and in shoulder lanes, since this is the information that is typically required by Alberta Transportation in bridge inspections conducted in the province.

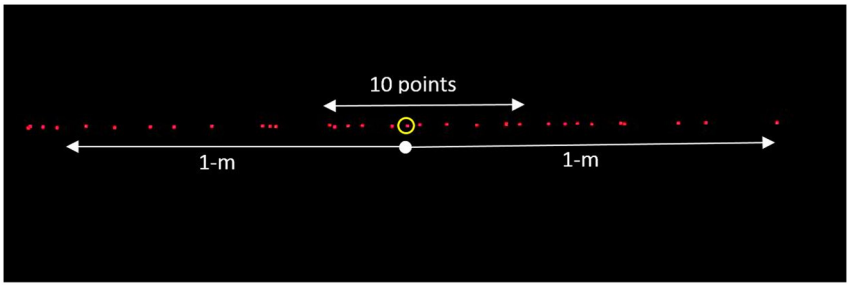

Fig. 7. Assessing the existence of other overhead points within the vicinity of the detected overhead point (Circled).

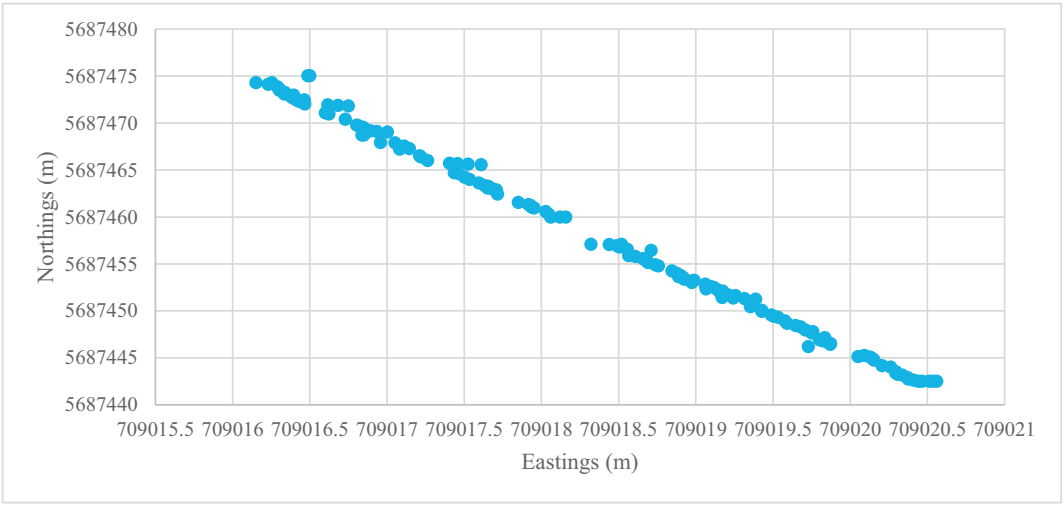

(a) Detected Points on Bridge

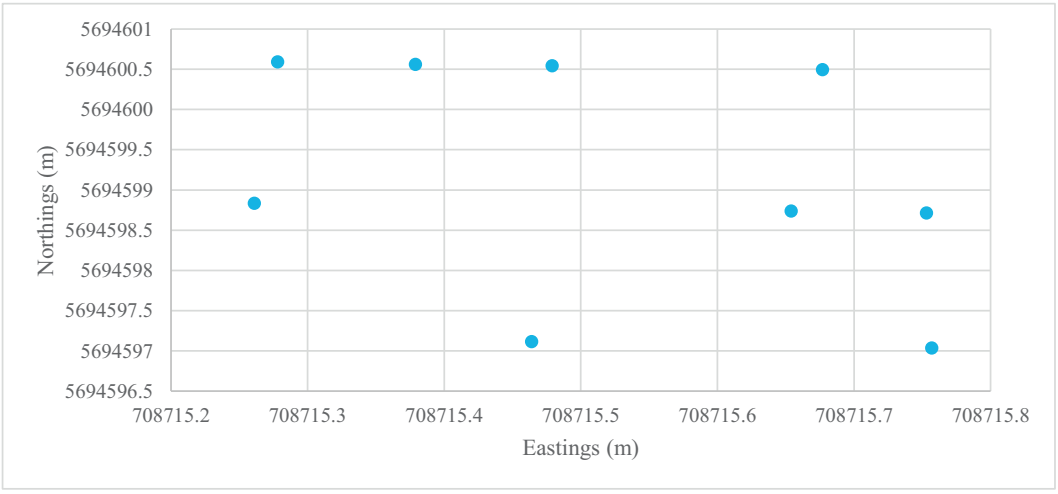

(b) Detected Points on a Powerline

Fig. 8. Points detected on overhead object.

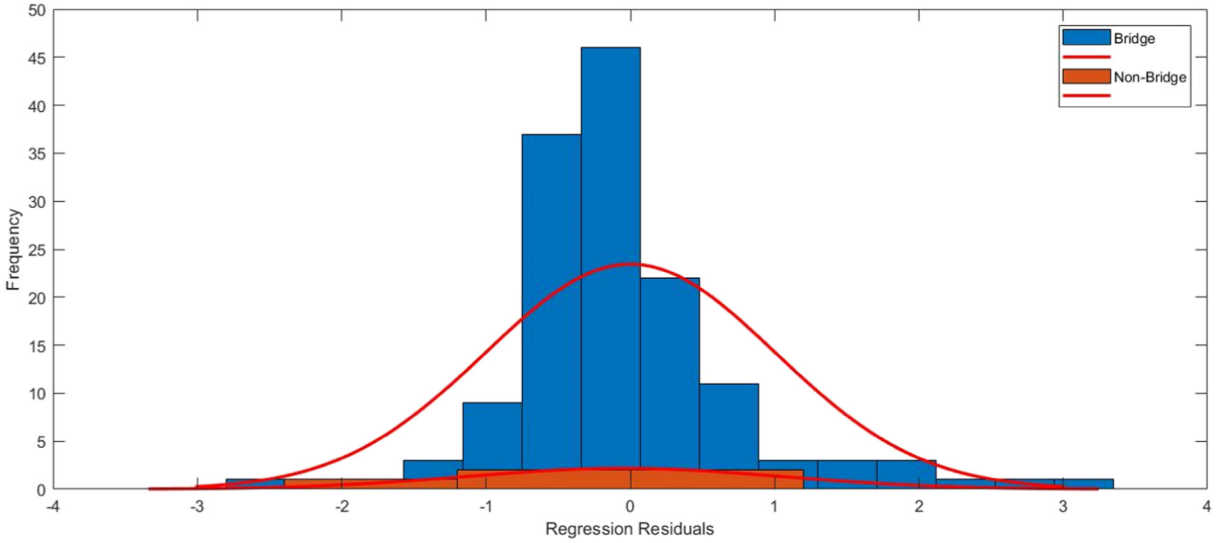

Fig. 9. Histogram of residuals (bridge vs non-bridge).

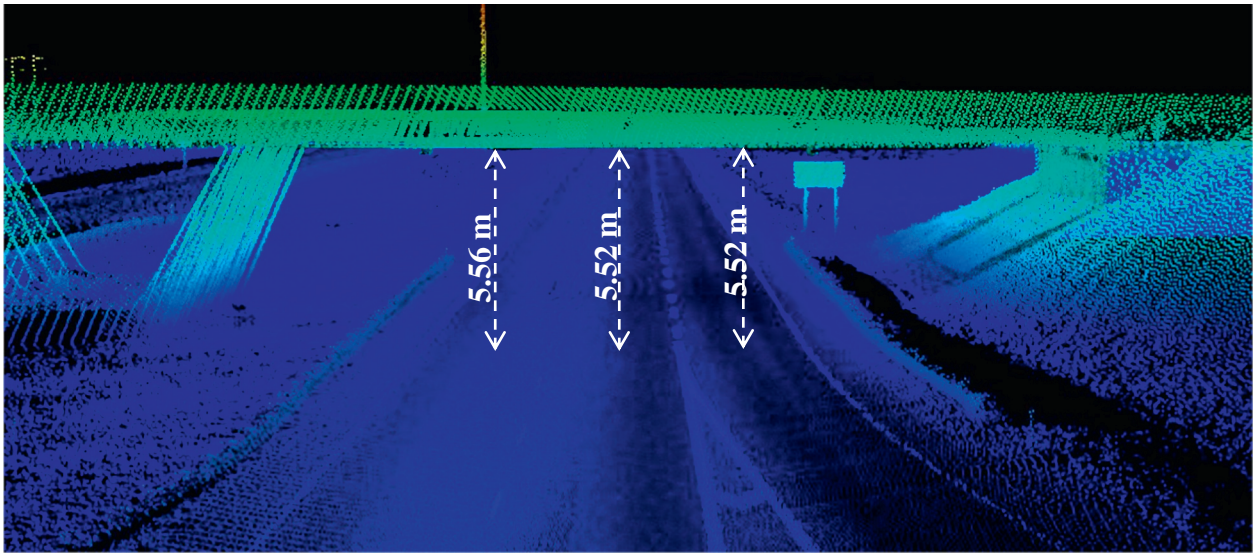

Fig. 10. Detailed clearance assessment highway 1 Bridge B.

4. Case study

The developed algorithm was tested on two different highways in the Province of Alberta, Canada. The two segments were both divided highway segments which included a variety of overhead structures including bridges, powerlines, cables and overhead signs. The segments had differing levels of vegetation and tree density as well as different horizontal and vertical alignments. The next few paragraphs provide information about the data collection process along with some details about the two highways on which the proposed algorithm was tested.

4.1. LiDAR data collection

The LiDAR data used in this study was collected by Alberta Transportation in surveys conducted on multiple highways across the province. In mobile laser scanning (MLS) a data collection vehicle is mounted with a laser scanning system. The laser scanner can be mounted to any vehicle with a roof rack. The vehicle then travels highway corridors at highway speeds of up to 100 km/h to collect the data creating a 360° point cloud of the road's environment. Unlike static terrestrial scans where a significant amount of time is required to set up scanning equipment and relocating from one bridge to another, the fact that mobile LiDAR can be collected while travelling at highway speeds helps improve the efficiency of the data collection process. It also minimizes the disruption caused to traffic since road closure is not required when mobile LiDAR is collected.

The MLS system used to collect data for this study was the RIEGL VMX-450. Among other components, the RIEGL VMX-450 system is equipped with two VQ-450 scanners and IMU/GNSS units (Inertial Measurement Unit/Global Navigation Satellite System). The laser scanners are symmetrically configured on the left and right sides, pointing toward the rear of the vehicle at a heading angle of approximately 145°. The VQ-450 scanner has a scan rate of up to 1.1 million points per second and a scan speed of 400 lines per second, a precision of 5 mm and an accuracy of 8 mm [39]. The density of the points on a scanned object depends on the range, and the speed of the data collection truck. Provincial surveys conducted at 90 km/h result in LiDAR point densities on the pavement surface of 100–1000 points/m^2 [40].

Data collected along a given highway is saved in multiple *.LAS* files with each file representing a certain segment along the highway. Due to the high point density of the data, the size of the 4 km segment file could reach over 500 MB. The data considered in this paper was collected on the three different segments shown in Fig. 11.

Data considered in this paper was collected on three different highways in Alberta, Canada. Clearance information on each of the three highways was obtained using the proposed method. For two of the test highways, the extracted information was compared to clearance information posted at bridges. For a short segment on the third highway, the extracted information was compared to clearance information obtained in bridge inspections conducted by Alberta Transportation (Alberta's Department of Transport).

4.1.1. Highway 1

The portion of Highway 1 (also known as the Trans-Canada Highway) considered in the analysis extends a length of 4 km and lies in the western part of the Province of Alberta, Canada. The segment is part of a 4-lane divided highway located west of the City of Calgary. The speed limit on the segment is 110 km/h and it is highly travelled due to its proximity to the Banff National Park. The segment also has a high density of trees and vegetation on either side of the road as seen in Fig. 11a. In addition, there is physical separation of the two travel approaches. The type of median varies along the segment (depressed vs. raised) as does the horizontal alignment of the segment. Two interchanges exist on the segment. The point cloud file of this segment consisted of over 17 million points. Overhead structures on this segment included two bridges in addition to several power lines and overhead signs.

4.1.2. Highway 14

The Highway 14 segment extended a length of 4 km. This segment was also a 4-lane divided rural road. The highway is located southeast of the City of Edmonton in Alberta, Canada. The travel approaches are separated by a depressed median with moderate vegetation and tree density on the side of the road as seen in Fig. 11b. It is worth noting that part of this segment has travel approaches which are completely separated as the highway merges into the Anthony Henday drive which is a major ring-road circulating the City of Edmonton. The LiDAR point cloud file for this segment consisted of 31.7 million points. The speed limit on the road is 100 km/h. Four different bridges exist on the analyzed portion of this segment as well as a number of power lines.

4.1.3. Highway 2 (corridor assessment)

The section of Highway 2 (also known as the Queen Elizabeth II Highway) considered in the analysis lies in the central part of the Province of Alberta. The segment is part of a 4-lane divided highway located in between the cities of Calgary and Edmonton. The speed limit

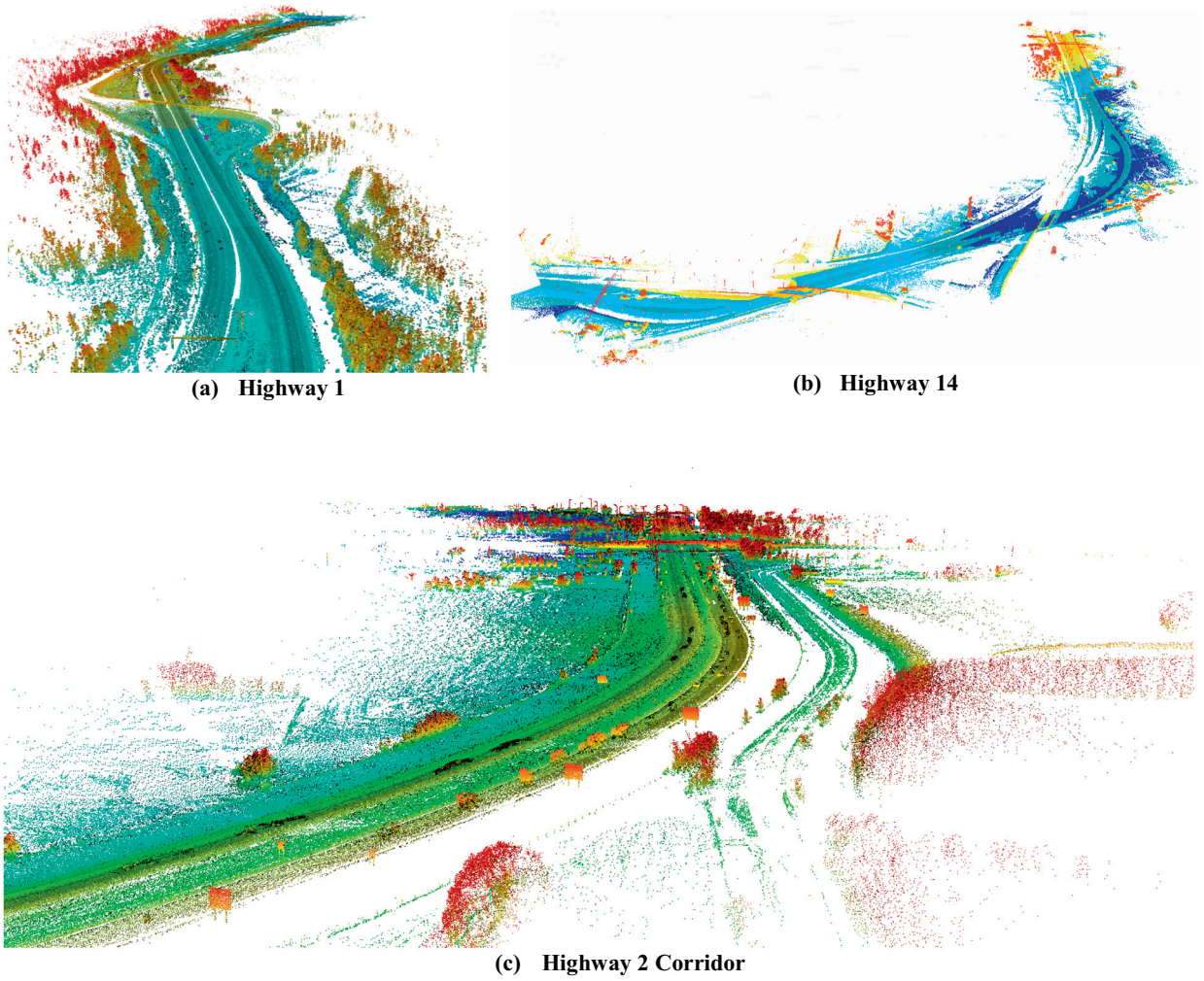

(a) Highway 1

(b) Highway 14

(c) Highway 2 Corridor

Fig. 11. Point cloud data at test highways.

on the segment is 110 km/h and it is highly travelled as it is the main transportation route connecting Northern and Southern Alberta. The segment is primarily bordered by low vegetation as seen in Fig. 11c. In addition, there is physical separation of the two travel approaches. The median varies along the segment (depressed vs. raised) as does the horizontal alignment of the segment. This Highway was used for two purposes, the proposed algorithm was used to estimate clearance and detect overhead objects for the entire highway corridor which extended a length of 242 km. The 242-km segment consists of over 1 billion points resulting in 41 GB of raw LiDAR data. For one bridge along the highway corridor clearance information collected by Alberta Transportation in a Bridge inspection report was available, hence, this information was used to validate the clearance assessments obtained using the proposed algorithm.

4.2. Result assessment metrics

To numerically assess the validity of the results, three metrics (precision, detection rate, and accuracy) were calculated. The metrics were calculated as follows:

$$\text{Precision} = \frac{TP}{TP + FP} \tag{9}$$

$$\text{Detection Rate} = \frac{TP}{TP + FN} \tag{10}$$

$$\text{Accuracy} = \frac{TP + TN}{TP + FN + FP + TN} \tag{11}$$

where, TP and TN denote the number of true positives and the true negatives. FP denotes the number of false positives and FN denotes the number of false negatives.

Accuracy measures how effective the algorithm is in the valid classification of both true positives and true negatives, this measure is also known as *quality* and provides a compound performance metric that balances detection rate and precision [41]. *Detection rate*, also known as *completeness*, measures how effective the algorithm is in the valid identification of true positives only. Finally, *Precision*, also known as *correctness*, measures how successful the algorithm is in applying the classification filters.

5. Results and discussion

5.1. Overhead object detection

For further testing and validation of the repeatability of the proposed method. The algorithm was tested on LiDAR data collected on Highways 1, 2, and 14. On Highway 1 and 14, testing was conducted on short subsegments of the highways (around 4 km each), whereas for Highway 2 testing was carried out on the entire highway corridor that extended 242 km between Alberta's most populous cities Edmonton and Calgary.

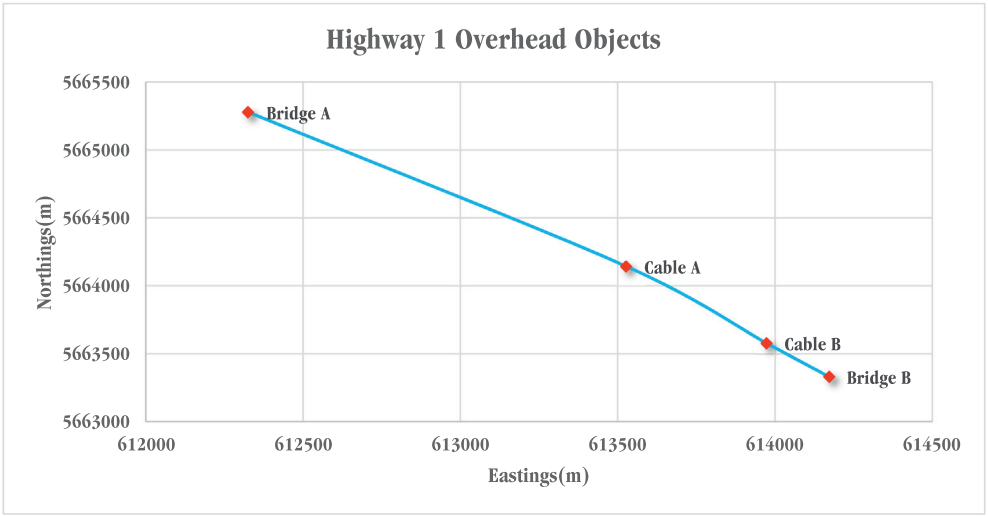

(a) Detection Results

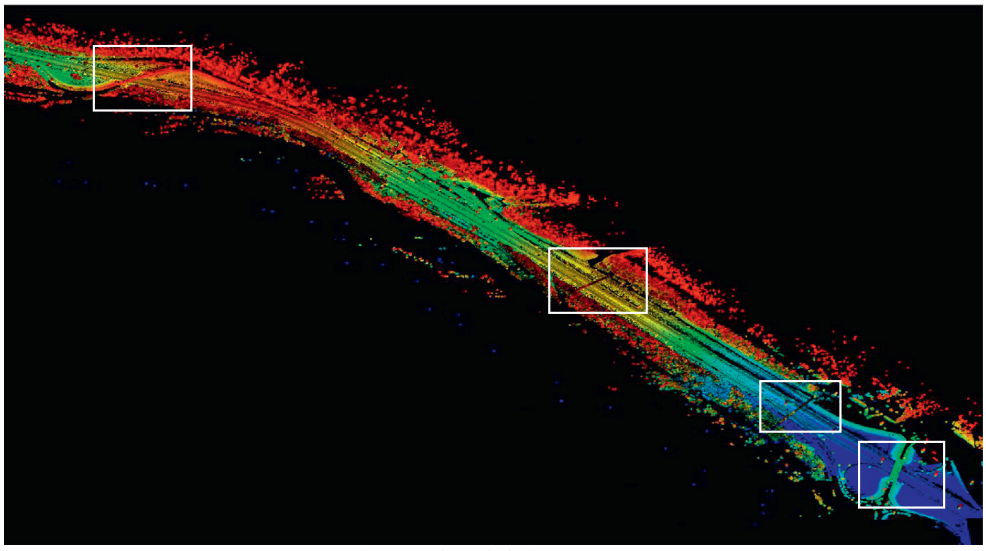

(b) Plan view of LiDAR segment

Fig. 12. Overhead structures detected on highway 1.

5.1.1. Short test segments

Figs. 12 and 13 show the results of the overhead structure detection performed on both Highway 1 and 14, respectively. For each highway, two different figures are displayed. The top figures (Figs. 12a and 13a) represents a plot of the detected clusters and the bottom figures (Figs. 12b and 13b) represents a plan view of the point cloud data. The horizontal axis on the plots represents the Universal Transverse Mercator (UTM) easting coordinates while the vertical axis represents the UTM northing coordinates. Each diamond on the plots represents a cluster of points which, in turn, represent a single overhead structure. If the cluster on Figs. 12a and 13a are traced down to Figs. 12b and 13b the overhead object can be seen on the plan view of the LiDAR highway.

Tables 1 and 2 also show the overhead structure detection results for Highways 1 and 14, respectively. For each of the detected clusters, the tables show the cluster ID, the overhead object each cluster represents, the coordinates of the object, the minimum elevation and the points per cluster.

On the analyzed segment of Highway 1, four different overhead structures existed, namely; two bridges and two powerlines. On Highway 14, there were six different overhead objects on the analyzed segment - two pairs of bridges and two powerlines. As evident in Tables 1, 3 and 4, the algorithm successfully detected all overhead structures on all three test segments.

5.1.2. Long highway corridor

To demonstrate the repeatability of the proposed method and its efficiency in a large-scale assessment, the algorithm was used to detect overhead objects along the Highway 2 Corridor in central Alberta. The algorithm was successful in detecting all 152 objects that existed on the analyzed segment without any False Positives. This included single cable powerlines, multi-cable powerlines, overhead signs, and bridges. Although no false positives were detected (i.e. all 152 objects were accurately detected), the detection process did result in two false negatives (i.e. overhead objects that were not detected). These were a virtual weigh station cantilever and an overhead sign that extended onto a single lane of the highway. It is worth noting here that detecting those objects is possible by simply offsetting the trajectory defined in Section 3.1.1 to the lane of interest.

In addition to the accurate detection of objects, the algorithm was also successful in accurately classifying overhead objects into bridges and non-bridges. Out of 32 bridge structures on the 242 km of the

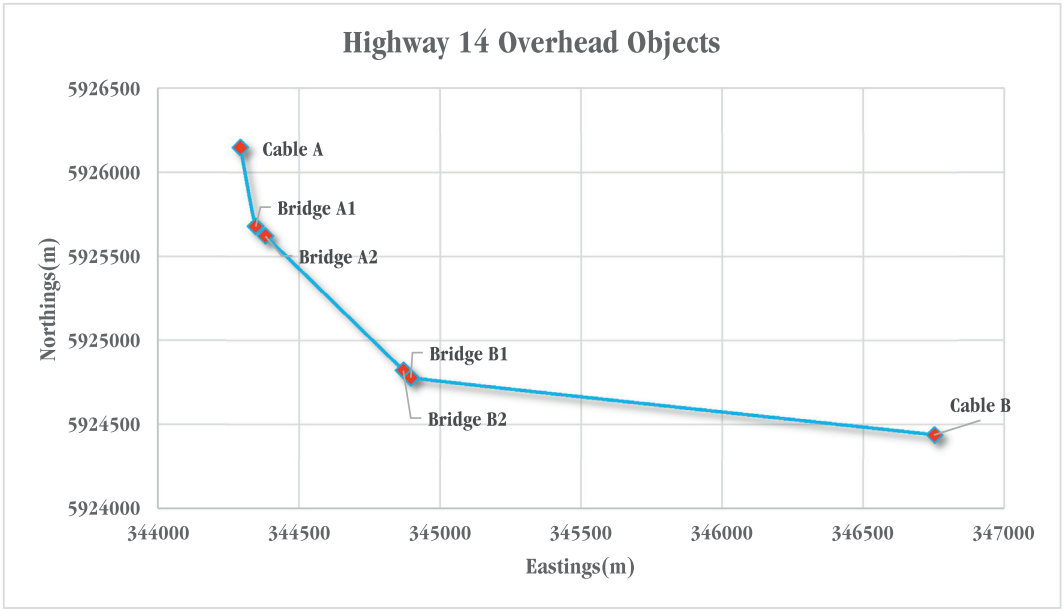

(a) Detection Results

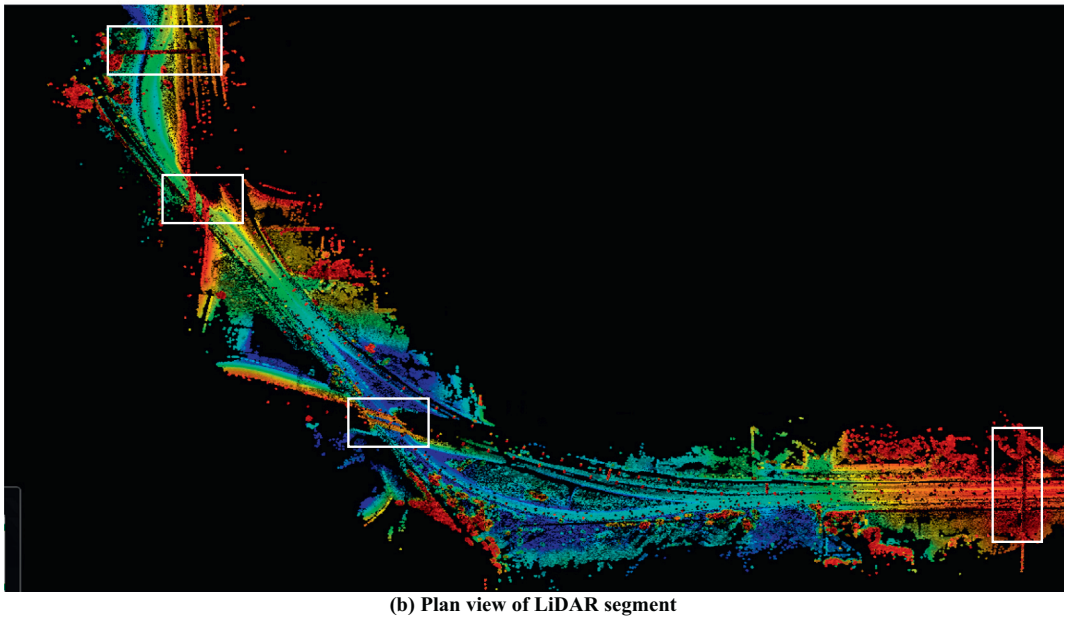

(b) Plan view of LiDAR segment

Fig. 13. Overhead structures detected on highway 1.

Table 1
Overhead object detection results (Highway 1).

Cluster ID	Object	Eastings	Northings	Min Clearance	Points per cluster
1	Bridge A	5,665,281	612,324.3	5.56	79
3	Cable A	5,664,144	613,526.5	6.91	24
4	Cable B	5,663,579	613,972.6	6.91	15
5	Bridge B	5,663,332	614,171.5	5.46	66

Table 2
Overhead object detection results (Highway 14).

Cluster ID	Object	Eastings	Northings	Clearance	Points per cluster
1	Cable	344,291.6	5,926,148	15.77	45
2	Bridge A1	344,345.6	5,925,679	6.03	154
3	Bridge A2	344,380.2	5,925,623	6.65	146
4	Bridge B1	344,869.3	5,924,822	5.76	158
5	Bridge B2	344,895.9	5,924,779	5.85	173
6	Cable	346,752.7	5,924,438	14.3	33

highway, the classification process yielded 4 false negatives and 2 false positives. Two of the false negatives (i.e. overhead objects that were classified into non-bridges despite representing bridge structure) were incomplete bridges that were split between two LiDAR segments due to the way the LAS files were stored. This causes the number of points on the bridge structure to get split between two sections. Another false negative was a pedestrian footbridge, which did not have a span as wide as traffic bridges. As for the false positives, one of those was a powerline that consisted of over 10 cables, which resulted in a point density similar to that of a bridge. Although these powerlines are rare, they could be distinguished from bridges due to the high clearance at those objects (typically > 11 m).

Table 3
Result validity assessment.

Metric	Detection of overhead objects	Classification of objects
Precision (%)	100	93.8
Detection rate (%)	98.7	88.2
Accuracy (%)	98.7	96.3

Table 4
Clearance verification results.

Lane position[a]	Span direction/ number[b]	Clearance measured during bridge inspection	Clearance obtained using proposed method	Difference (cm)
L1	S3N	6.41	6.396	1.4
LS	S3N	6.65	6.619	3.1
RS	S3N	6.17	6.155	1.5
L1	S3S	6.4	6.396	0.4
LS	S3S	6.65	6.619	3.1
RS	S3S	6.13	6.132	−0.2

[a] L: Left, R: Right, S:Shoulder.
[b] For span orientation, letter indicates span direction and number further specifies the location on the bridge, for further information see Chapter 7 of Alberta Transportation's Bridge Inspection Manual [43].

To numerically assess the validity of the results, three metrics (precision, detection rate, and accuracy) were calculated. These metrics were computed to assess the validity of both the detection process (i.e. the accuracy of the proposed algorithm in detecting all overhead objects on the test highway), and the classification process (i.e. the ability of the proposed method in accurately classifying detected overhead objects into bridges and non-bridges). The metrics for detection and classification are presented in Table 3.

The high percentages in table, combined with the fact that these results were obtained on a long highway corridor illustrate the robustness of the proposed method in detecting and classifying overhead objects. The results show the ability of the algorithm in accurately detecting and classifying overhead objects regardless of the length of the highway, or the type of overhead objects that exist on the highway.

5.2. Clearance assessment

5.2.1. Preliminary clearance estimate

As already noted, a preliminary estimate for clearance at each overhead object is obtained as part of the detection process described in Section 3.1.3. The preliminary clearance estimates obtained on the Highway 1 and Highway 14 test segments are presented in Tables 1 and 2 are first explored. For Highway 1, the minimum bridge clearance based on the detection results is 5.56 m and 5.46 m for Bridges A and B, respectively. On Highway 14, the minimum clearance was 5.76 m and 5.85 m for Bridges A1 and A2 and 6.65 m and 6.03 m for the two Bridges B1 and B2.

The posted minimum clearance at the analyzed bridges, as shown in Table 5 (columns 6) ranges from 5.2 m to 6.5 m. It is worth noting that Alberta Transportation require that the posted minimum clearance is 0.1-m less than the minimum height measured between the lowest point on the overhead structure and the surface of the roadway. After subtracting the 0.1 m tolerance, the number is also rounded down to the nearest 0.1 m. This means that if the minimum clearance measured at a bridge is 5.32 m, the posted minimum clearance beneath the bridge should be 5.2 m.

After comparing the minimum clearance based on the posted information to that obtained from the detection, the results reveal that the percentage difference ranges from 0.69 to 3% with an average difference of 0.92% for all bridges. This indicates that even the clearance estimate obtained in the detection process is a good representation of the measured clearance at the bridge.

With regards to the power lines, the minimum clearances are also summarized in Tables 1 and 2. Clearance information about those objects is not known and not posted, however, clearance at powerlines typically ranges from 6 to 20 m depending on the voltage being carried in the cable [42]. This was indeed the case for all the powerlines that were detected in this paper.

5.2.2. Detailed clearance assessment

As highlighted in the last few paragraphs, the detection process proposed in this paper yields accurate estimates of clearance information at all the detected objects. These measurements eliminate the likelihood of human error associated with traditional surveying practice, thus, resulting in more accuracy. Nonetheless, if the absolute minimum clearance across the span of an overhead object is desired, a detailed clearance assessment is still required. Accordingly, the detailed assessment was performed at all the bridges detected in this paper due to their long span.

5.2.2.1. Clearance information validation. Before the detailed clearance assessment was conducted on Highway 1 and Highway 14, the clearance assessment procedure was tested along a subsegment of the Highway 2 corridor where ground truth clearance measurements were available. This was a 4 km segment that lies north of the town of Lacombe. The point cloud file for this segment consisted of 29.5 million points. Only one bridge existed on the analyzed segment, however, a power lines and an overhead sign were also present. For verification purposes, the results of the detailed clearance assessment obtained using the proposed method were compared to the information obtained by Alberta Transportation in bridge inspections. Table 4 shows the results of the comparison.

The differences in vertical clearance between the values measured in bridge inspection and those obtained using the proposed procedure suggest that the methodology is accurate in determining the vertical clearance. The differences in clearance range from 0.4 to 3.1 cm, which could be caused by human error or potential imperfections when conducting manual field measurements. These differences translate to percent differences that range from 0.03 to 0.47%, which indicates a high level of accuracy.

Table 5
Clearance assessment results.

	LiDAR detailed assessment				Conventional measure		Difference in clearance
	Average	Min 10%	Min 5%	Min	Posted	Calculated	Posted – detailed clearance measure (cm)
HWY 1 Bridge A	6.31	5.54	5.49	5.45	5.30	5.40	15.30
HWY 1 Bridge B	6.33	5.61	5.58	5.52	5.30	5.40	21.70
HWY 14 Bridge A1	7.51	6.10	6.05	6.03	5.90	6.00	13.20
HWY 14 Bridge A2	8.10	6.73	6.67	6.65	6.50	6.60	15.10
HWY 14 Bridge B1	7.07	5.78	5.77	5.74	5.70	5.80	4.00
HWY 14 Bridge B2	7.16	5.85	5.84	5.79	5.70	5.80	8.70

Fig. 14. Steel girders below bridge deck.

5.2.2.2. Clearance compared to posted clearance information. The results of the detailed clearance assessment on highways 1 and 14 are shown in Table 5. For these bridges ground truth information was not available since no bridge inspections took place at those locations, however, the results were compared to the posted clearance information. Table 5 shows the average clearance obtained from multiple points across each bridge's deck, the average of the minimum 10%, the average of the minimum 5% and the absolute minimum clearance value.

As evident by the difference between the average clearance (column 2) and the absolute minimum clearance (column 5) in Table 5, the clearance observations vary significantly beneath the bridges. The lower deck of the bridge contains steel girders which cause the observed variations in the vertical clearance, as seen in Fig. 14. The variation is also due to the slopes of the roadway or the overpass itself. Such variations highlight the importance of obtaining multiple clearance observations below a bridge's deck to increase the likelihood of finding the 'true' minimum clearance.

The actual minimum clearance obtained using the LiDAR assessment on all highways was conservative (i.e. the posted clearance was still less than the actual minimum obtained from the LiDAR analysis). Nonetheless, the differences between the absolute minimum clearance obtained at some of the bridges and the minimum clearance sign posted at those bridges was relatively close. For instance, at Bridge B1 on Highway 14 the posted clearance was only 4 cm lower than the absolute minimum obtained in the assessment procedure. While such a difference might be acceptable, it shows that DOTs must be extra cautions when posting minimum clearance signs.

As already noted in the paper, AT requires that a 10 cm margin of safety is used when deciding on the minimum clearance that must be posted at a particular bridge. Accordingly, the posted clearance is expected to be 10 to 15 cm less than the absolute minimum clearance measured at the bridge. While this is the case for most of the bridges assessed in this paper, the fact that this is not the case for Bridges B1 and B2 on Highway 14 indicates that the posted clearance was based on a clearance value which was not the absolute minimum at the bridge.

This finding demonstrates the importance of performing a detailed assessment of clearance before posting clearance signs as an error of 5 to 10 cm in the posted clearance might be the difference between a truck driving smoothly beneath a bridge and a collision costing hundreds of thousands of dollars in repairs.

The assessment also shows that if it is evident that on multiple bridges the posted clearance is not based on the absolute minimum, due to limitations in conventional clearance measurement tool, DOT's still using those tools might need to revise the margin of error used when posting minimum clearance signs.

5.3. Processing time

The process proposed in this study for overhead object detection, classification and clearance assessment takes approximately 1 min/km for a Desktop PC with Intel i7 CPU and 16 GB RAM. This could vary depending on the number of overhead objects on a segment, however, the estimate is based on analysis conducted in this study, which includes 242 km of the Highway 2 corridor (the longest and busiest highway in the province of Alberta) where 152 overhead objects exist (0.62 objects per km). It has been reported in previous research, based on data from Washington State DOT, that manual clearance assessment of a single bridge can take up to 1.5 h, which excludes relocation time from one structure to another, lodging time and expenses for surveying crew [8]. Therefore, the proposed method creates significant time savings for agencies interested in assessing clearance information along highways. Furthermore, the fact that the same LiDAR dataset could be used for multiple applications helps save time spent in field visits collecting other information about road infrastructure [44].

6. Conclusions and recommendations

This study provides a novel algorithm which can be used to efficiently assess vertical clearance on a highway network using LiDAR point cloud data. The algorithm involves automatically detecting, classifying and assessing the vertical clearance at all overhead objects on a highway. The proposed technique provides an exhaustive and accurate method for the assessment of vertical clearance in much safer conditions than existing techniques.

The proposed algorithm was tested using data collected on three highways in the Province of Alberta, Canada including a 242 km highway corridor. The results of the analysis showed that the algorithm was successful in detecting the vast majority of overhead objects on all highways. This included the detection of powerline cables, overhead signs and bridges. Furthermore, comparison of the clearance information obtained using the proposed method to those documented in bridge inspection reports revealed that the proposed method provides an extremely accurate clearance measurement, with percent differences of $< 0.47\%$.

One limitation of the proposed method lies in its inability to detect powerlines with a very low point density. Although the algorithm checks LiDAR points within the lateral vicinity of powerlines of low density (Section 3.1.3), there are some instances where even lateral point density (i.e. the point density across the length of the powerline) is sparse. This makes it difficult to distinguish such objects from noise in the data. Although this did not significantly impact the quality of the results, future studies might need to consider region growing techniques to overcome the issue of sparse point density along those power lines. Another challenge which may hinder the assessment process in some cases is the existence of incomplete overhead objects. This is either caused by object occlusion during data collection (which is highly unlikely since the main source of occlusion is typically vehicles travelling on the highway which cannot obstruct overhead objects due to the difference in height) or LiDAR scan segmentation. LiDAR data collected on a highway is often broken down into several subsegments of manageable size. Breaking down those segments sometimes occurs at interchanges and results in the bridges at those interchanges getting split into two segments. This impacts the accuracy of the classification process of the detected overhead asset. Therefore, it is recommended that such segmentation is avoided if the datasets are to be used for clearance assessment.

Despite these challenges, this paper demonstrates that the developed algorithm is of great value for transportation agencies looking to automatically inventory and classify overhead objects on an entire highway network with minimal effort. The efficiency with which clearance can be assessed using the proposed algorithm makes it extremely valuable when network-level assessment of clearance is desired. Bridge management agencies can also use the extracted information as part of their routine inspection of bridges to help manage their rehabilitation and maintenance programs. The extracted information could help agencies prioritize structures with significant clearance problems which would lead to agencies addressing integrity concerns in a timely manner before irreversible damage occurs or safety problems arise. The proposed detailed clearance assessment of bridges also increases the likelihood of detecting the absolute minimum clearance beneath a structure, which is not always possible using manual procedures. As evident in the paper, the absolute minimum clearance might be relatively close to the posted clearance in some cases. If this is observed at multiple locations on a highway network, agencies might consider updating design codes to incorporate higher margins of safety when posting clearance information based on manually measured clearance estimates.

Acknowledgments

The authors would like to thank Alberta Transportation for sponsoring and providing the data used in this study. Acknowledgments are also extended to Alberta Innovates and Alberta Advanced Education for the financial support.

References

[1] A.C. Estes, D.M. Frangopol, Updating bridge reliability based on bridge management systems visual inspection results, J. Bridg. Eng. 8 (6) (2003) 374–382, https://doi.org/10.1061/(ASCE)1084-0702(2003)8:6(374).
[2] B. Riveiro, D. Jauregui, P. Arias, J. Armesto, R. Jiang, An innovative method for remote measurement of minimum vertical underclearance in routine bridge inspection, Autom. Constr. 25 (2012) 34–40, https://doi.org/10.1016/j.autcon.2012.04.008.
[3] V. Gattulli, L. Chiaramonte, Condition assessment by visual inspection for a bridge management system, Comput. Aided Civ. Infrastruct. Eng. 20 (2) (2005) 95–107, https://doi.org/10.1111/j.1467-8667.2005.00379.x.
[4] S. Gargoum, L. Karsten, K. El-Basyouny, Network level clearance assessment using LiDAR to improve the reliability and efficiency of issuing over-height permits on highways, Transp. Res. Rec. (2018), https://doi.org/10.1177/0361198118758687.
[5] B. Nguyen, I. Brilakis, Understanding the Problem of Bridge and Tunnel Strikes Caused by Over-height Vehicles, (2016), https://doi.org/10.1016/j.trpro.2016.05.481.
[6] FHWA, F.H. Adminstration (Ed.), Interstate System Conditions and Performance, 2013.
[7] J. Wang, X. Ye, Application of Laser Collision Avoidance System for Crossroads, Beijing Evening 485, (2007) http://news.sina.com.cn/c/2007-07-31/143012303005s.shtml.
[8] K.S. Yen, T.A. Lasky, B. Ravani, Cost-benefit analysis of mobile terrestrial laser scanning applications for highway infrastructure, J. Infrastruct. Syst. 20 (4) (2014) 04014022, , https://doi.org/10.1061/(ASCE)IS.1943-555X.0000192.
[9] R. Vasquez, "Endeavour" Moves Through the Cloud, vol. 2018, (2012).
[10] Alberta Transportation, Budget 2016 Highlights, vol. 2016, Government of Alberta, 2016.
[11] T.F. Fwa, The Handbook of Highway Engineering, CRC Press, 9781420039504, 2005.
[12] A. Hammad, J. Yan, B. Mostofi, Recent development of bridge management systems in Canada, 2007 Annual Conference and Exhibition of the Transportation Association of Canada: Transportation-An Economic Enabler (Les Transports: Un Levier Economique), 2007.
[13] A. Transportation, T.I.M. System (Ed.), Existing Structures in the Provincial Highway Corridor, Alberta Transportation, 2017, p. 328.
[14] FHWA, N.B.I. U.S. Federal Highway Administration (Ed.), State Bridge Inspection Data, Structurally Deficient Ratings, 2013.
[15] W. Liu, S.-e. Chen, E. Hasuer, Bridge clearance evaluation based on terrestrial LIDAR scan, J. Perform. Constr. Facil. 26 (4) (2012), https://doi.org/10.1061/(ASCE)CF.1943-5509.0000208.
[16] K. Williams, M.J. Olsen, G.V. Roe, C. Glennie, Synthesis of transportation applications of mobile LiDAR, Remote Sens. 5 (9) (2013) 4652–4692, https://doi.org/10.3390/rs5094652.
[17] M. Soilán, B. Riveiro, J. Martínez-Sánchez, P. Arias, Traffic sign detection in MLS acquired point clouds for geometric and image-based semantic inventory, ISPRS J. Photogramm. Remote Sens. 114 (2016) 92–101, https://doi.org/10.1016/j.isprsjprs.2016.01.019.
[18] H. Guan, J. Li, Y. Yu, C. Wang, M. Chapman, B. Yang, Using mobile laser scanning data for automated extraction of road markings, ISPRS J. Photogramm. Remote Sens. 87 (2014) 93–107, https://doi.org/10.1016/j.isprsjprs.2013.11.005.
[19] C. Ai, Y.J. Tsai, An automated sign retroreflectivity condition evaluation methodology using mobile LIDAR and computer vision, Transp. Res. Part C Emerg. Technol. 63 (2016) 96–113, https://doi.org/10.1016/j.trc.2015.12.002.
[20] L. Truong-Hong, D.F. Laefer, T. Hinks, H. Carr, Combining an angle criterion with voxelization and the flying voxel method in reconstructing building models from LiDAR data, Comput. Aided Civ. Infrastruct. Eng. 28 (2) (2013) 112–129, https://doi.org/10.1111/j.1467-8667.2012.00761.x.
[21] A. Holgado-Barco, B. Riveiro, D. González-Aguilera, P. Arias, Automatic inventory of road cross-sections from mobile laser scanning system, Comput. Aided Civ. Infrastruct. Eng. 32 (1) (2017) 3–17, https://doi.org/10.1111/mice.12213.
[22] A. Holgado-Barco, D. González-Aguilera, P. Arias-Sanchez, J. Martinez-Sanchez, Semiautomatic extraction of road horizontal alignment from a mobile LiDAR system, Comput. Aided Civ. Infrastruct. Eng. 30 (3) (2015) 217–228, https://doi.org/10.1111/mice.12087.
[23] P. Kumar, C.P. McElhinney, P. Lewis, T. McCarthy, An automated algorithm for extracting road edges from terrestrial mobile LiDAR data, ISPRS J. Photogramm. Remote Sens. 85 (2013) 44–55, https://doi.org/10.1016/j.isprsjprs.2013.08.003.
[24] S. Gargoum, K. El-Basyouny, Automated extraction of road features using LiDAR data: a review of LiDAR applications in transportation, 4th International Conference on Transportation Innovation and Safety (ICTIS), IEEE, 2017, pp. 563–574, , https://doi.org/10.1109/ICTIS.2017.8047822.
[25] B. Riveiro, M. DeJong, B. Conde, Automated processing of large point clouds for structural health monitoring of masonry arch bridges, Autom. Constr. 72 (2016) 258–268, https://doi.org/10.1016/j.autcon.2016.02.009.
[26] J. Guo, M.-J. Tsai, J.-Y. Han, Automatic reconstruction of road surface features by using terrestrial mobile lidar, Autom. Constr. 58 (2015) 165–175, https://doi.org/10.1016/j.autcon.2015.07.017.
[27] S. Gargoum, K. El-Basyouny, J. Sabbagh, Automated extraction of horizontal curve

attributes using LiDAR data, Transp. Res. Rec. 0 (0) (2018), https://doi.org/10.1177/0361198118758685 0361198118758685.
[28] M. Castro, L. Iglesias, J.A. Sánchez, L. Ambrosio, Sight distance analysis of highways using GIS tools, Transp. Res. Part C Emerg. Technol. 19 (6) (2011) 997–1005, https://doi.org/10.1016/j.trc.2011.05.012.
[29] S. Gargoum, K. El-Basyouny, J. Sabbagh, Assessing stopping and passing sight distance on highways using mobile LiDAR data, J. Comput. Civ. Eng. (2018), https://doi.org/10.1061/(ASCE)CP.1943-5487.0000753 10.1061/(ASCE)CP.1943-5487.0000753.
[30] Alberta Transportation, Vertical Clearance Measurements (VCL2), Alberta Infrastructure and Transportation, 2014, p. 13.
[31] R.G. Lauzon, Automated Vertical Clearance Measurement during Photolog Operations, (2000).
[32] I. Puente, B. Akinci, H. González-Jorge, L. Díaz-Vilariño, P. Arias, A semi-automated method for extracting vertical clearance and cross sections in tunnels using mobile LiDAR data, Tunn. Undergr. Space Technol. 59 (2016) 48–54, https://doi.org/10.1016/j.tust.2016.06.010.
[33] P. Nourian, R. Gonçalves, S. Zlatanova, K.A. Ohori, A.V. Vo, Voxelization algorithms for geospatial applications: computational methods for voxelating spatial datasets of 3D city models containing 3D surface, curve and point data models, MethodsX 3 (2016) 69–86, https://doi.org/10.1016/j.mex.2016.01.001.
[34] C.E. Prakash, S. Manohar, Volume rendering of unstructured grids—a voxelization approach, Comput. Graph. 19 (5) (1995) 711–726, https://doi.org/10.1016/0097-8493(95)00053-4.
[35] N.S. Altman, An introduction to kernel and nearest-neighbor nonparametric regression, Am. Stat. 46 (3) (1992) 175–185, https://doi.org/10.1080/00031305.1992.10475879.
[36] M. Ester, H.-P. Kriegel, J. Sander, X. Xu, A density-based algorithm for discovering clusters in large spatial databases with noise, Kdd 96 (1996) 226–231 (10.1.1.121.9220).
[37] D.S. Moore, S. Kirkland, The Basic Practice of Statistics, WH Freeman, New York, 2007.
[38] S.P. Washington, M.G. Karlaftis, F.L. Mannering, Statistical and Econometric Methods for Transportation Data Analysis, Chapman and Hall/CRC, 9781420082852, 2003.
[39] RIEGL, RIEGL VMX-450 Data Sheet, RIEGL Laser Measurement Systems, 2015.
[40] P. Steel, D. Mesher, J. Adamson, Development of a road safety audit network screening tool, Twenty-Fourth Canadian Multidisciplinary Road Safety Conference, 2014.
[41] M. Rutzinger, F. Rottensteiner, N. Pfeifer, A comparison of evaluation techniques for building extraction from airborne laser scanning, IEEE J. Sel. Top. Appl. Earth Obs. Remote. Sens. 2 (1) (2009) 11–20, https://doi.org/10.1109/JSTARS.2009.2012488.
[42] OPSD, O.P.S. Drawing (Ed.), Minimum Vertical Clearances for Areial Cable System, Ontario Department of Transport, Ontario, 2011.
[43] Alberta Transportation, A. Transportation (Eds.), Bridge Inspection Manual - Vertical Clearance Measurements, 7–8 2004, pp. 7–10.
[44] J. Chang, D. Findley, C. Cunningham, M. Tsai, Considerations for effective lidar deployment by transportation agencies, Transp. Res. Rec. J. Transp. Res. Board 2440 (2014) 1–8, https://doi.org/10.3141/2440-01.